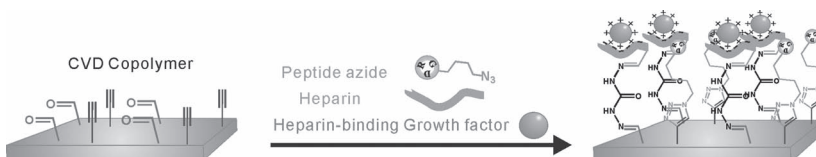


A Generic Strategy for Co-Presentation of Heparin-Binding Growth Factors Based on CVD Polymerization

Xiaopei Deng, Joerg Lahann*

A multifunctional copolymer with both aldehyde and alkyne groups is synthesized by chemical vapor deposition (CVD) for orthogonal co-immobilization of biomolecules. Surface analytical methods including FTIR and XPS are used to confirm the surface modification. Heparin-binding growth factors [basic fibroblast growth factor (bFGF) in this study] can be immobilized through interaction with heparin, which was covalently attached to the CVD surface through an aldehyde-hydrazide reaction. In parallel, an alkyne-azide reaction is used to orthogonally co-immobilize an adhesion peptide as the second biomolecule.



1. Introduction

Precise surface engineering is one of the major challenges in biotechnology.^[1] While it is widely recognized that the fate of cells cultured *in vitro* is determined by their local microenvironment consisting of both soluble and solid components, many biological studies focus mainly on the role of soluble factors, which can be controlled by simple methods.^[2,3] However, the defined presentation of biomolecules on the cell culture substrates can contribute in equal ways to a specific cellular response.^[1,4] For example, extracellular matrix proteins, such as fibronectin, laminin, or collagen, are routinely attached to cell culture dishes to facilitate cell adhesion.^[5,6] While there exists a multitude of immobilization methods for single biomolecules,^[7] these

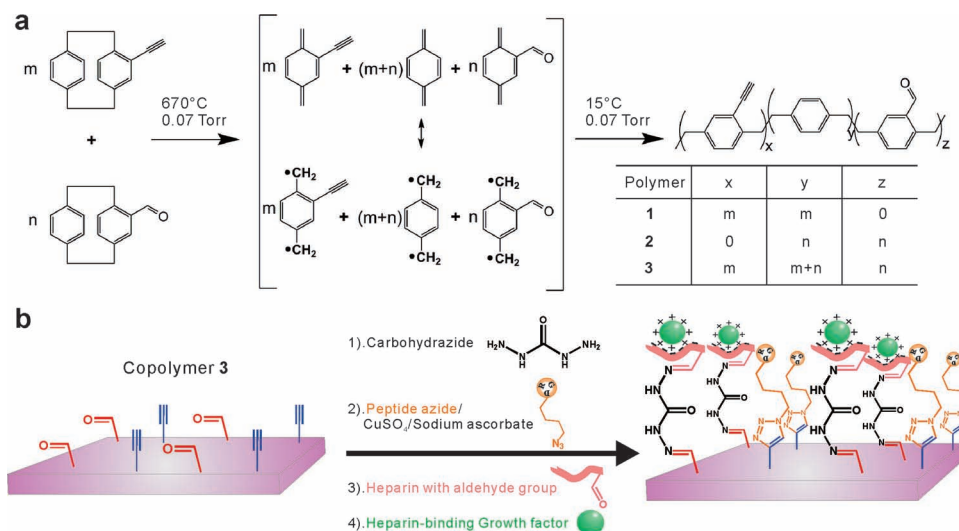
approaches typically do not account for the multivalency of biological interactions. Controlled co-immobilization of multiple biomolecules is an essential requisite for certain biomedical applications, such as *in vitro* cell culture or biosensors.^[8–10] If proteins are immobilized through simple physisorption, the outcomes are governed by complex adsorption/desorption equilibria.^[1] If multiple proteins are presented on a surface, the physisorption dynamics are governed by the Vroman effect leading to a continuous exchange of proteins until coverage with the largest protein is obtained.^[11] Thus, physisorption methods are unable to precisely engineer stable protein compositions on a surface. Alternatively, chemical immobilization can be employed. Simultaneous presentation of multiple biomolecules to a substrate with a single surface chemistry (e.g., via active esters) has been previously reported.^[8,9] However, this method is still not precise, as the cross-reactivity of the biomolecules may be associated with a range of different complications. For example, the solution composition of the biomolecules is not necessarily the final composition encountered on the surface after immobilization.

A more appropriate approach is the use of orthogonal immobilization strategies, where a substrate presents multiple types of functional groups without cross-reactivity.^[12–14] Recently, we have established an orthogonal co-immobilization method for the cyclic RGD (cRGD) adhesion peptide and the epidermal growth factor

X. Deng

Macromolecular Science and Engineering,
University of Michigan, Ann Arbor, MI 48109, USA
Prof. Dr. J. Lahann

Departments of Chemical Engineering, Materials Science
and Engineering, Macromolecular Science and Engineering
and Biomedical Engineering, University of Michigan, Ann
Arbor, MI 48109, USA; Institute of Functional Interfaces,
Karlsruhe Institute of Technology, Hermann-von-Helmholtz-
Platz 1, 76344 Eggenstein-Leopoldshafen, Germany
E-mail: lahann@umich.edu



Scheme 1. a) CVD copolymerization of [2.2]paracyclophanes with aldehyde and alkyne groups. $m = n$ for the copolymer 3 discussed in this paper. Polymer 1 and 2 are used as controls. b) Co-immobilization scheme for heparin-binding growth factor and adhesion peptide on the copolymer 3.

(EGF), which uses chemical vapor deposition (CVD) copolymerization of two different functionalized [2.2]paracyclophanes yielding a polymer surface that presented acetylene and pentafluorophenol ester groups in an equimolar ratio.^[13] In this case, coupling of the peptide was achieved via copper-catalyzed heterocycloaddition and the growth factor was linked through primary amino groups via pentafluorophenol ester groups. In our previous studies, we found that the choice of pentafluorophenol ester groups is lacking specificity towards the growth factor because of the abundance of amino groups in biomolecules. We also found that the immobilization of proteins through potentially vital amino acids can potentially reduce their bioactivity.^[15] Whether or not the direct immobilization via primary amino groups is applicable will thus need to be validated on a case-by-case basis for each different growth factor. In addition, the direct immobilization approach does not reflect the fact that growth factors immobilized on abiotic surfaces can easily undergo denaturation and that the use of appropriate linkers may effectively stabilize the immobilized growth factors.

In this paper, we develop a generic immobilization approach for heparin-binding growth factors, which includes numerous commonly used growth factors, such as fibroblast growth factors (FGFs), vascular endothelial growth factor, heparin-binding EGF-like growth factor (HB-EGF), platelet-derived growth factor, or hepatocyte growth factor (HGF). As an example, we selected the basic fibroblast growth factor (bFGF) as a model of a heparin-binding growth factor. However, we note that the herein developed procedure is equally applicable to other heparin-binding growth factors. It has been previously reported that binding to heparin protects FGF from denaturation at variant pH, at

high temperatures, and proteolysis.^[16–18] Moreover, binding either to heparin or heparan sulfate is a prerequisite for the binding of FGF to its high-affinity receptor on the cell surface.^[19] Considering the importance of heparin for protecting bFGF and enhancing its bioactivity, we designed a method to first immobilize heparin on the surface and then tether the growth factor through the heparin-binding domain and charge interactions.^[20] We further demonstrate the compatibility of this approach with the co-immobilization of an additional biological moiety via the well established and widely employed copper-catalyzed heterocycloaddition.^[13,21] However, the CVD coatings may carry a wide range of different functional groups including anhydrides, active esters, aldehydes, ketones, amines, alkyne, as well as photo-reactive benzoyl groups.^[22]

2. Experimental Section

2.1. Materials

All materials were purchased from Sigma–Aldrich and used without further purification unless otherwise indicated.

2.2. CVD Co-Polymerization

The synthesis of the two CVD precursors used in this study, 4-formyl[2.2]paracyclophane and 4-ethynyl[2.2]paracyclophane was described elsewhere.^[22,23] As shown in Scheme 1a, CVD co-polymerization was performed using 1:1 molar mixtures of the two precursors. The precursors sublimated under 0.07 Torr at temperatures above 100 °C and were transferred in a stream of argon carrier gas (20 sccm) to the pyrolysis zone (670 °C). Following pyrolysis, the diradicals were transferred into the

deposition chamber, with the chamber wall temperature set at 120 °C and rotating sample holder cooled to 15 °C to optimize the deposition. The coatings were controlled at 80–100 nm.

2.3. Surface Characterization

FTIR analysis of the coatings was carried out on a Nicolet 6700 spectrometer with the MCT-A detector and the grazing angle accessory (Smart SAGA) at a grazing angle of 80°. XPS was performed on an axis ultra X-ray photoelectron spectrometer (Kratos Analyticals, UK) equipped with a monochromatized Al-K α X-ray source. All spectra were calibrated with respect to the non-functionalized aliphatic carbon with a binding energy of 285.0 eV. An imaging spectroscopic ellipsometer (Accurion, Nanofilm EP³-SE, Germany) was used to measure film thickness. Ellipsometric parameters were fitted using a Cauchy model.^[24] The imaging lateral resolution is $\approx 2 \mu\text{m}$ for the 10 \times objective. Time-of-flight secondary ion mass spectrometry (TOF-SIMS) was performed on a PHI TRIFT V nanoTOF instrument (Physical Electronics, USA). The analysis conditions are the following: primary ion 30 kV Au⁺, DC current 2.5 nA, mass range 0–1850 m/z , analysis area 400 $\mu\text{m} \times 400 \mu\text{m}$ (256 \times 256 pixels), charge compensation 15 eV e⁻, post acceleration 5 kV, acquisition time 10 min ($< 1 \times 10^{11}$ ions cm^{-2}) per data set. Data was collected in both ion polarities in an automated fashion using AutoTool. The diagnostic mass peaks were observed $< 300 m/z$.

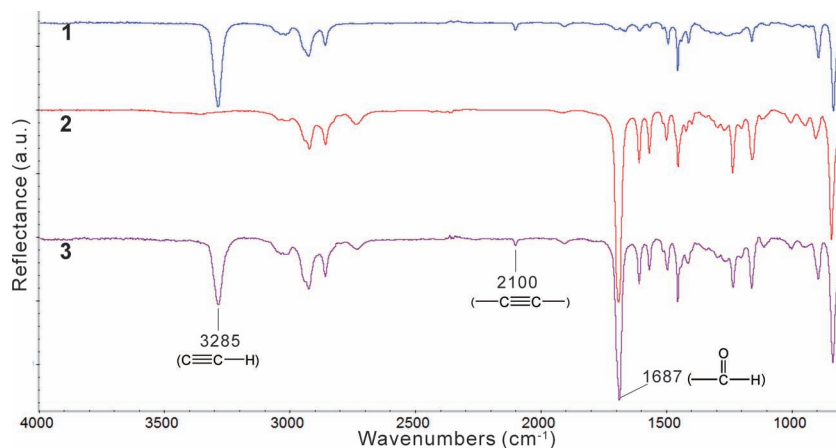
2.4. Immobilization of Biomolecules

The details and sequence for co-immobilization of the adhesion peptide and the heparin-binding growth factor are shown in Scheme 1b. Microcontact printing (μCP) with PDMS stamps (preparation process reported elsewhere^[22]) was used for elucidating the surface chemistries and creating internal reference areas that can be directly observed by microscopy. The method for adhesion peptide immobilization followed a literature-known procedure.^[13] Briefly, rRGD peptide with an azide end group [cyclo(azidoK-RGDf), Kinexus, Canada] was dissolved in an aqueous solution of sodium ascorbate (50 mg mL^{-1}) and copper(II) sulfate ($0.1 \times 10^{-3} \text{M}$). The peptide solution (50 $\mu\text{g mL}^{-1}$) was in contact with the CVD copolymer coating (polymer **3**) for 4 h followed by thorough washing. For the heparin immobilization, the periodated heparin (Celsus Laboratories, Inc.) with aldehyde functional groups was used. A bivalent carbohydrazide linker was used to link the aldehyde groups on the polymer surface and heparin. The PDMS stamps inked with carbohydrazide solution (10 $\mu\text{g mL}^{-1}$) were kept in contact with the coating surface for 20 min. After stamp removal, the patterned samples were thoroughly washed with distilled water and incubated in the periodated heparin solution (10 mg mL^{-1} , pH 5) overnight. To confirm the success of the heparin immobilization, immunostaining was performed with the heparin antibody (anti-heparin/Heparan Sulfate, clone T320.11, Isotype: mouse IgG1, Millipore) and the Alexa Fluor[®] 555 anti-mouse IgG1 (Life Technologies Corporation).

More specifically, the surface was incubated in a heparin antibody solution (5 $\mu\text{g mL}^{-1}$ solution in PBS with 0.1% (w/v) bovine albumin (BSA) and 0.02% (v/v) Tween 20 for 1 h. After washing thoroughly, the surface was incubated in a PBS/BSA/Tween buffer containing Alexa Fluor[®] 555 anti-mouse IgG1 (10 $\mu\text{g mL}^{-1}$) for 1 h. The stained samples were then washed with PBS, rinsed with distilled water, and visualized using fluorescence microscopy (Olympus BX-51, Japan). For immobilization of the human bFGF (Sigma–Aldrich) on heparin, a heparin-presenting surface (without antibody) was incubated in the PBS/BSA/Tween buffer containing bFGF (5 $\mu\text{g mL}^{-1}$) for 1 h and washed thoroughly. To confirm the success of the bFGF immobilization, immunostaining was performed, as described for heparin. The only difference was that instead of using heparin antibody, we used an anti-human bFGF (Isotype: mouse IgG1, BioLegend) as the primary antibody. Other conditions (buffer, concentration, incubation time, secondary antibody, and washing procedure) were identical.

3. Results and Discussion

A novel polymer coating with orthogonal functional groups, poly[4-formyl-*p*-xylylene-co-4-ethynyl-*p*-xylylene-co-*p*-xylylene] (polymer **3**), was synthesized by CVD copolymerization as shown in Scheme 1a. The precursors 4-ethynyl[2,2]paracyclophane and 4-formyl[2,2]paracyclophane were sublimated with a controlled feed ratio ($m:n$, $m = n$ in this study). The mixture was then transferred through the pyrolysis zone (670 °C, 0.07 Torr) with help of an argon carrier gas. Free radicals were generated by pyrolysis and subsequently deposited and polymerized on the cooled substrate (15 °C, 0.07 Torr). Under these reaction conditions, CVD co-polymerization yielded polymer **3** as shown in Scheme 1. Polymers **1** and **2**, which are shown for comparison, denote polymers generated using only one precursor and thus featuring only one reactive functional group (alkyne for **1**; aldehyde for **2**). **1**, **2**, and **3** were characterized by Fourier transform infrared (FTIR) spectroscopy (Figure 1) and X-ray photoelectron spectroscopy



■ Figure 1. FTIR spectra for polymers **1**, **2**, and **3**.

Table 1. Chemical composition of polymers **1**, **2**, and **3** in at% shown as experimental values determined by XPS. Theoretically calculated compositions are included for comparison.

	C—C/H	C—C=O	C=O	$\pi\rightarrow\pi^*$	O
B.E. [eV]	285.0	285.7 ± 0.1	287.7 ± 0.1	291.3 ± 0.1	532^{a)}
1	94.7 (100.0)	— (—)	— (—)	4.0 (—)	1.3 (—)
2	75.7 (83.2)	6.7 (5.6)	5.8 (5.6)	4.3 (—)	7.5 (5.6)
3	85.6 (91.6)	3.5 (2.8)	3.1 (2.8)	4.0 (—)	3.8 (2.8)

^{a)}Experimental values of oxygen ratio [%] are from survey results; Other experimental values for different carbon atoms with different chemical states are from high resolution C1s spectra.

(XPS) (Table 1). It is clearly shown from the FTIR spectra that **3** has both alkyne (3285 , 2100 cm^{-1}) and aldehyde (1687 cm^{-1}) functional groups, while **1** or **2** displays only one type of functional groups. XPS was used to further confirm the surface composition of the films within the outermost 10 nm.^[25] The percentage of total carbon and oxygen was obtained from the XPS survey results. High resolution peak fitting of the C1s signal was used to determine the ratios of different carbon atoms at different chemical states. The position for C—C/H was set to be 285.0 eV for binding energy calibration. Other carbon atoms with different chemical states have different binding energies as shown in Table 1. The quantitative XPS experimental data were in good agreement with the theoretical values calculated according to the chemical structures of the starting materials (Scheme 1a).

After confirming the successful preparation of the multifunctional reactive coating, each step for the biomolecules immobilization had to be validated. The overall design for our co-immobilization process is shown in Scheme 1. Heparin was immobilized on the copolymer surface through the hydrazide–aldehyde reaction, which is highly efficient, commonly used for bioconjugation and classified as one of the bioorthogonal reactions.^[14]

Carbohydrazide with a hydrazide group on both ends was used to link the aldehyde group of heparin and the aldehyde group on the copolymer **3** surface. To confirm that the carbohydrazide is indeed attached to the surface through covalent reaction, we conducted a ToF-SIMS study. ToF-SIMS is a surface-sensitive analytical tool that provides information on the uppermost few molecular layers. ToF-SIMS has been previously used in materials science,^[26,27] semiconductor industry,^[28,29] geology,^[30] archaeometry,^[31] cosmochemistry,^[32] and biology.^[33,34] The mass imaging capability of ToF-SIMS combines the potential benefits of chemical imaging and mass spectroscopy.^[35] Sample surfaces in this study were coated with the copolymer **3** and then modified by microcontact printing of the carbohydrazide linker. The resultant patterns were clearly observable in the ToF-SIMS images. For all the images shown in Figure 2a, the brighter areas were patterned with carbohydrazide, while the darker areas were not (with only the copolymer **3** coating). Signals at m/z 26 and 42, which corresponded to CN^- and CNO^- signals were predominantly observed within the area patterned with carbohydrazide. Since the polymer itself does not have any nitrogen, the nitrogen-containing mass peaks can be exclusively attributed to the presence of the

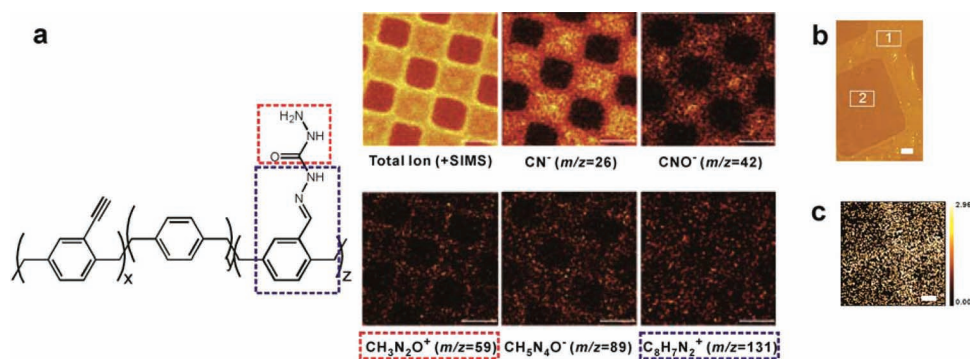


Figure 2. a) TOF-SIMS images of carbohydrazide patterned on polymer **3**. The m/z values and their corresponding chemical structures are denoted by squares of different colors. b) Imaging ellipsometry thickness map of carbohydrazide pattern by μCP , the thickness difference between the marked area 1 and 2 is 0.3 nm. c) Imaging XPS N1s elemental map of the carbohydrazide pattern at 400.0 eV. All scale bars represent 50 μm .

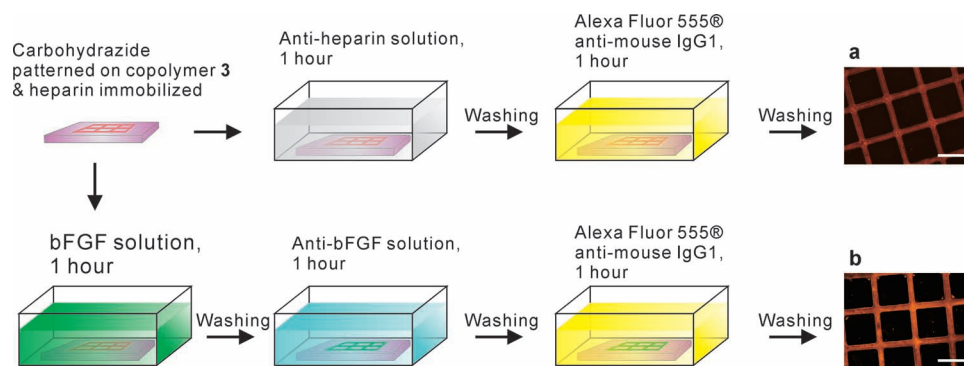


Figure 3. Scheme and fluorescence microscope images (a & b) after immunostaining the heparin and bFGF immobilized surface, respectively. In the scheme for this Figure, we use pink to represent heparin and green to represent bFGF, the same colors used in Scheme 1b. a) Fluorescence micrograph after immunostaining the immobilized heparin on the patterned carbohydrate. b) Fluorescence micrograph after immunostaining the immobilized bFGF on the heparin. Scale bars are 500 μm .

carbohydrazide. Similarly, mass peaks of m/z 59 and 89, which are characteristic fragments of the carbohydrate linker, are significantly enhanced in the surface-modified areas. Moreover, the mass fragment m/z 131, which coincides with the m/z 59 signal further supports the formation of a covalent bond between the linker and the polymer, albeit with lower contrast. Imaging ellipsometer was also used to investigate thickness variations after carbohydrate patterning (Figure 2b). The film thickness of the carbohydrate immobilized onto copolymer **3** was measured to be 0.3 nm. For comparison, microcontact printing of carbohydrate onto polymer **1** was used as a control experiment, which showed no patterns based on imaging ellipsometry (data not shown). This contrast clearly demonstrates the orthogonality of the surface chemistries (i.e., alkyne–azide reaction versus aldehyde–hydrazide reaction). Moreover, XPS mapping of the element nitrogen (Figure 2c), which was used as a reporter for the carbohydrate linker, further confirmed the ToF-SIMS results. A cross pattern is shown in Figure 2c. The relatively low signal-to-noise ratio in the XPS mapping experiment can be attributed to the overall low content of nitrogen on the surface (less than 3%). Still, taken together, the images shown in Figure 2 confirm that the carbohydrate was covalently attached to the copolymer **3** through the aldehyde–hydrazide reaction.

A surface displaying carbohydrate patterns was incubated in periodated heparin (with aldehyde groups) solution overnight followed by thorough rinsing with distilled water. After this heparin immobilization step, a heparin antibody and a dye-conjugated secondary antibody were used for immunostaining (Figure 3, top scheme). From the image shown on the top right of Figure 3, it is evident that heparin was immobilized only at the surface areas that presented carbohydrate. Two control experiments were performed. For the first one, we used a carbohydrate

patterned surface (without the heparin immobilization step) for the immunostaining. For the second control experiment, the heparin-presenting surface was in contact with the secondary antibody only, but not the primary antibody (anti-heparin). Both control experiments did not show fluorescence contrast for the patterns (data not shown).

After validating the heparin immobilization approach, the heparin-presenting surface was incubated in a bFGF solution (Figure 3, bottom scheme), followed by washing and bFGF immunostaining. The bottom right fluorescence micrograph in Figure 3 shows that bFGF was only immobilized at the area that presented heparin. Again, we included two control experiments to validate the bFGF immunostaining. First, the surface was patterned with carbohydrate (no heparin immobilization), followed by the same bFGF incubation and immunostaining shown as in the bottom scheme of Figure 3. Second, we performed every immobilization step for carbohydrate, heparin and bFGF, but omitted the primary antibody. With other words, the resultant surface was only in contact with the secondary antibody. Both control experiments did not show fluorescence contrast for the patterns (data not shown). For the heparin and the bFGF immunostaining, we used different primary antibody (heparin antibody and bFGF antibody, respectively). Because both antibodies belong to the isotype mouse IgG1 family, we were able to image both with the same secondary antibody (Alexa Fluor® 555 anti-mouse IgG1), hence the identical colors in Figure 3. Nevertheless, a clear contrast is observed in both cases confirming the selectivity of both reactions. At this point, we have established the success of each immobilization step towards tethering the heparin-binding growth factor. We finally wanted to establish co-immobilization with a second coupling biomolecule, specifically cRGD, via azide–acetylene coupling.

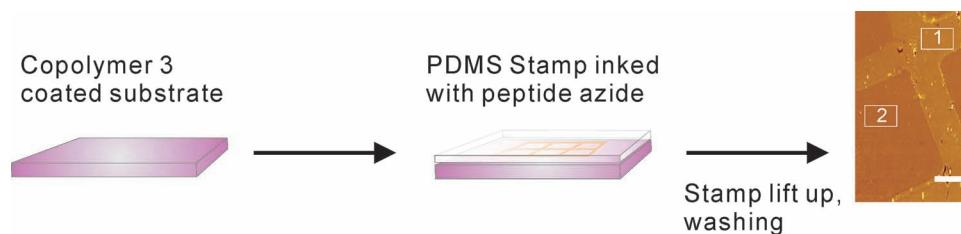


Figure 4. Imaging ellipsometry thickness map (on the right side) of a cRGD azide pattern created by μ CP. The thickness difference between the marked area 1 and 2 is 0.5 nm. Scale bar represents 100 μ m.

The results for patterning an azide-functionalized cRGD peptide onto polymer **3** are shown in Figure 4. Imaging ellipsometry was used to generate the thickness map for the patterned adhesion peptide on the newly synthesized copolymer **3** (Figure 4). The immobilized peptide layer was measured to be 0.5 nm. A control experiment with the same peptide patterned on polymer **2** did not show any pattern contrast (data not shown). This again demonstrates the orthogonality of the alkyne–azide chemistry and the aldehyde–hydrazide chemistry we use. The alkyne–azide chemistry is chosen for immobilization of a second biomolecule, here a cyclic RGD (cRGD) peptide, because of its high efficiency and natural orthogonality to other commonly used bioconjugation chemistries.^[13]

4. Conclusions

We successfully prepared a new CVD copolymer for orthogonal co-immobilization of heparin-binding growth factors with an adhesion peptide. To establish a generic growth factor immobilization scheme, the CVD co-polymer was modified to allow for immobilization of heparin onto the surface. The presence of heparin leads to non-covalent binding of heparin-binding growth factors and can potentially enhance the bioactivity of the growth factor. In parallel, an adhesion peptide is also immobilized to the surface using orthogonal bioconjugation schemes. Due to the substrate-independent nature of the CVD polymerization process, this novel procedure is rather generic and can be widely applied as a surface engineering platform for a broad range of biomedical applications. Further biological studies are under way to identify the quantitative information about the co-immobilization ratios that will be associated with the highest biological activity in cell culture. We note that the biomolecules that can be orthogonally immobilized via the herein reported procedure are not limited to adhesion peptides and growth factors. While other biomolecules such as enzymes, antibodies, or polysaccharides are also compatible with this approach, this strategy is not suitable for co-immobilization of multiple heparin-binding growth factors. In this case, more traditional orthogonal immobilization strategies will need to be employed.^[13]

Acknowledgements: We thank Dr. Gregory L. Fisher at Physical Electronics for the ToF-SIMS experiment and data analysis. The authors gratefully acknowledge support from Army Research Office (ARO) Grant W911NF-11-1-0251.

Received: May 16, 2012; Revised: June 26, 2012; Published online: August 7, 2012; DOI: 10.1002/marc.201200343

Keywords: biomaterials; biomolecules; coatings; immobilization; surface engineering

- [1] D. G. Castner, B. D. Ratner, *Surf. Sci.* **2002**, *500*, 28.
- [2] S. Maeno, Y. Niki, H. Matsumoto, H. Morioka, T. Yatabe, A. Funayama, Y. Toyama, T. Taguchi, J. Tanaka, *Biomaterials* **2005**, *26*, 4847.
- [3] W. R. Walsh, N. Guzelsu, *Biomaterials* **1993**, *14*, 331.
- [4] Y. Ito, *Soft Matter* **2008**, *4*, 46.
- [5] M. Attia, J. P. Santerre, R. A. Kandel, *Biomaterials* **2011**, *32*, 450.
- [6] R. O. Hynes, *Cell* **1992**, *69*, 11.
- [7] T. Ahuja, I. A. Mir, D. Kumar, Rajesh, *Biomaterials* **2007**, *28*, 791.
- [8] H. Hatakeyama, A. Kikuchi, M. Yamato, T. Okano, *Biomaterials* **2007**, *28*, 3632.
- [9] H. Teymourian, A. Salimi, R. Hallaj, *Biosens. Bioelectron.* **2012**, *33*, 60.
- [10] A. Sassolas, L. J. Blum, B. D. Leca-Bouvier, *Biotechnol. Adv.* **2012**, *30*, 489.
- [11] L. Vroman, A. L. Adams, G. C. Fischer, P. C. Munoz, *Blood* **1980**, *55*, 156.
- [12] C. Wendeln, S. Rinnen, C. Schulz, T. Kaufmann, H. F. Arlinghaus, B. J. Ravoo, *Chem. Eur. J.* **2012**, *18*, 5880.
- [13] X. Deng, T. W. Eyster, Y. Elkasabi, J. Lahann, *Macromol. Rapid Comm.* **2012**, *33*, 640.
- [14] E. M. Sletten, C. R. Bertozzi, *Angew. Chem. Int. Ed.* **2009**, *48*, 6974.
- [15] J. Lahann, W. Pluster, T. Rodon, M. Fabry, D. Klee, H. G. Gattner, H. Hocker, *Macromol. Biosci.* **2002**, *2*, 82.
- [16] D. Gospodarowicz, J. Cheng, *J. Cell. Physiol.* **1986**, *128*, 475.
- [17] S. Vemuri, I. Beylin, V. Sluzky, P. Stratton, G. Eberlein, Y. J. Wang, *J. Pharm. Pharmacol.* **1994**, *46*, 481.
- [18] A. Sommer, D. B. Rifkin, *J. Cell. Physiol.* **1989**, *138*, 215.
- [19] A. Yayon, M. Klagsbrun, J. D. Esko, P. Leder, D. M. Ornitz, *Cell* **1991**, *64*, 841.
- [20] L. D. Thompson, M. W. Pantoliano, B. A. Springer, *Biochemistry-Us* **1994**, *33*, 3831.
- [21] H. Nandivada, H. Y. Chen, L. Bondarenko, J. Lahann, *Angew. Chem. Int. Ed.* **2006**, *45*, 3360.
- [22] H. Y. Chen, J. Lahann, *Langmuir* **2011**, *27*, 34.

- [23] H. Nandivada, H. Y. Chen, J. Lahann, *Macromol. Rapid Comm.* **2005**, *26*, 1794.
- [24] J. Lahann, R. Langer, *Macromolecules* **2002**, *35*, 4380.
- [25] Y. Elkasabi, J. Lahann, *Macromol. Rapid Comm.* **2009**, *30*, 57.
- [26] A. Leute, D. Rading, A. Benninghoven, K. Schroeder, D. Klee, *Adv. Mater.* **1994**, *6*, 775.
- [27] B. Hagenhoff, A. Benninghoven, K. Stoppeklanger, J. Grobe, *Adv. Mater.* **1994**, *6*, 142.
- [28] I. Mowat, P. Lindley, L. McCaig, *Appl. Surf. Sci.* **2003**, *203*, 495.
- [29] B. A. Keller, P. Hug, *Anal. Chim. Acta* **1999**, *393*, 201.
- [30] X. Q. Hou, D. Y. Ren, H. L. Mao, J. J. Lei, K. L. Jin, P. K. Chu, F. Reich, D. H. Wayne, *Int. J. Coal Geol.* **1995**, *27*, 23.
- [31] D. S. McPhail, *Appl. Surf. Sci.* **2006**, *252*, 7107.
- [32] T. Stephan, *Planet. Space Sci.* **2001**, *49*, 859.
- [33] A. Brunelle, O. Laprevote, *Curr. Pharm. Des.* **2007**, *13*, 3335.
- [34] J. S. Fletcher, *Analyst* **2009**, *134*, 2204.
- [35] T. L. Colliver, C. L. Brummel, M. L. Pacholski, F. D. Swanek, A. G. Ewing, N. Winograd, *Anal. Chem.* **1997**, *69*, 2225.